Parasitol Res (2011) 109:941–947
DOI 10.1007/s00436-011-2314-7

SHORT COMMUNICATION

Merozoite release from *Plasmodium falciparum*-infected erythrocytes involves the transfer of $DiIC_{16}$ from infected cell membrane to Maurer's clefts

Gladys T. Cortés · Maria L. Caldas · Sonia J. Rahirant

Received: 17 December 2010 / Accepted: 24 February 2011 / Published online: 1 April 2011

Abstract Merozoite release from infected erythrocytes is a complex process, which is still not fully understood. Such process was characterised at ultra-structural level in this work by labelling erythrocyte membrane with a fluorescent lipid probe and subsequent photo-conversion into an electron-dense precipitate. A lipophilic $DiIC_{16}$ probe was inserted into the infected erythrocyte surface and the transport of this phospholipid analogue through the erythrocyte membrane was followed up during 48 h of the asexual erythrocyte cycle. The lipid probe was transferred from infected erythrocyte membranes to Maurer's clefts during merozoite release, thereby indicating that these membranes remained inside host cells after parasite release. Fluorescent structures were never observed inside infected erythrocytes preceding merozoite exit and merozoites released from infected erythrocyte were not fluorescent. However, specific precipitated material was localised bordering the parasitophorous vacuole membrane and tubovesicular membranes when labelled non-infected erythrocytes were invaded by merozoites. It was revealed that lipids were interchangeable from one membrane to another, passing from infected erythrocyte membrane to Maurer's clefts inside the erythrocyte ghost, even after merozoite release. Maurer's clefts became photo-converted following merozoite release, suggesting that these structures were in close contact with infected erythrocyte membrane during merozoite exit and possibly played some role in malarial parasite exit from the host cell.

Electronic supplementary material The online version of this article (doi:10.1007/s00436-011-2314-7) contains supplementary material, which is available to authorized users.

G. T. Cortés
Cell Biology Group, Public and Tropical Health Department, Faculty of Medicine, Universidad Nacional de Colombia, Bogotá, Colombia

G. T. Cortés
Biophysics Laboratory, Physics International Centre (CIF), carrera 30 calle 45, edificio Manuel Ancízar, ciudad universitaria, Bogotá, Colombia

M. L. Caldas
Cell Morphology Group, Instituto Nacional de Salud, Av. Calle 26 No. 51-60, Bogotá, Colombia
e-mail: mlcaldas@ins.gov.co

S. J. Rahirant
Cell Biochemistry Biology Group, Instituto Nacional de Salud, Bogotá, Colombia

G. T. Cortés (✉)
Departamento de Salud Pública y Tropical, Facultad de Medicina, Universidad Nacional de Colombia, Carrera 30 No. 45-03, edificio 471, oficina 145, 136 Bogotá, Colombia
e-mail: gtcortesc@unal.edu.co

Abbreviations

iE	Infected erythrocyte
iEM	Infected erythrocyte membrane
PVM	Parasitophorous vacuole membrane
PPM	Parasite plasmatic membrane
TVM	Tubovesicular membrane
TEM	Transmission electron microscopy
MC	Maurer's clefts

Introduction

The malarial parasite's complex life cycle involves a mosquito vector and a human host. *Plasmodium falciparum* resides within erythrocytes; parasite asexual replication

happens there resulting in merozoite production. Merozoites are released from infected erythrocytes (iE) and invade other erythrocytes, thereby repeating such asexual replication. A relatively clear picture has been emerging regarding the molecular mechanisms involved in merozoite invasion (Cowman and Crabb 2006); by contrast, no clear mechanism has emerged concerning how merozoites exit the erythrocyte (Rayner 2006).

Recently published film of merozoite release has suggested that merozoite exit involves an explosive event (Glushakova et al. 2005; Lew 2005; Rayner 2006); however, such film (Glushakova et al. 2005) is running around ten times faster than real time and the time between frames is several seconds. Winograd et al. (1999) have reported that merozoite clusters emerge from the erythrocyte in about 1 s.

Two main mechanisms have been implicated during parasite exit involving either rupture or membrane fusion (Rayner 2006); the former involves lysis of both the iE membrane and the parasitophorous vacuole membrane (PVM; Dvorak et al. 1975; Trager 2002; Salmon et al. 2001; Wickham et al. 2003; Glushakova et al. 2005). There is controversy regarding the role of the PVM and whether the PVM lyses concurrently with iE (Glushakova et al. 2005), beforehand (Wickham et al. 2003) or afterwards (Salmon et al. 2001; Soni et al. 2005). The second mechanism proposed for parasite exit involves PVM fusion with the iE membrane (Clavijo et al. 1998; Winograd et al. 1999, 2001). The present work was designed to show that iE cytoplasmatic content does not diffuse out as parasites are released; video microscopy was used to show that merozoites escaped from iE together with the hemozoin-containing residual body, leaving a membranous structure behind (Winograd et al. 1999). Interest was thus focused on determining how such mechanism acts during merozoite release from *P. falciparum*-iE.

This controversy has been partly due to the difficulty in studying merozoite release by existing microscope techniques. Efforts at understanding parasite exit have been hampered by the technical difficulties involved in working with membrane processes where membrane preservation in fixed parasites is generally poor. Most studies involve following individual iE by light microscope and little data is available at ultra-structural level (Glushakova et al. 2009, 2010; Salmon et al. 2001; Wickham et al. 2003). The present study examined a highly synchronised *P. falciparum*-iE population by transmission electron microscopy (TEM) during merozoite release and reinvasion and the fates of the iE membrane (iEM) after labelling with 1,1′-dihexadecyl-3,3′3,3′-tetramethylindocarbocyanine perchlorate ($DiIC_{16}$) fluorescent lipid probe, followed by photo-conversion.

Materials and methods

A highly synchronised *P. falciparum* (FCB-1 isolate)-iE culture was labelled with $DiIC_{16}$ lipid probe and kept in continuous culture as described by Trager and Jensen (1976); it was then examined by fluorescence and TEM following photo-conversion. Three rounds of sequential gelatin/sorbitol synchronisation involved synchronisation consisting of concentrating mature stage iE by gelatin flotation (Jensen 1978), returning iE to in vitro culture for 4 h and then subjecting them to sorbitol lysis (Lambros and Vanderberg 1979). The ring-iE obtained after the third synchronisation round were returned to culture for another 8–16 h, resulting in ring-stage parasites 12–20 h post-merozoite invasion. iE were then labelled with 0.5 μg/mL of $DiIC_{16}$ for 40 min at 37°C, in the dark, with continuous shaking. Precautions were taken to remove the probe which had not been inserted into the membrane to avoid possible spontaneous lipid transfer (Cohen and Melykian 1998). All labelled iE were then washed three times and returned to culture until the parasites were 42–44 h old; the medium was changed twice during this period. The cultures were monitored by using Giemsa staining until signs of reinvasion became evident; they were highly synchronous at this point to better enable observing merozoite release (Fig. 1). The 0.5 μg/mL $DiIC_{16}$ concentration did not affect parasite viability (data not shown), as described in Haldar and Uyetake (1992).

The labelled samples were collected during the period of maximum merozoite release and reinvasion. Samples were removed from culture and examined directly by bright field and fluorescent microscopy. A new method was standarized for studying complete vesicular and membrane material obtained during malarial parasite release from the host; such method was based on photobleaching *N*-[7-(4-nitrobenzo-2-oxa-1,3-diazole)] aminocaproyl sphingosine in *P. falciparum*-iE (Haldar et al. 1991), modified as described by Dantuma et al. (1998) and Maranto (1982). Examining ring-iE in recently reinvaded erythrocytes was used as control. All samples were examined after photo-conversion (Fig. 1); some were not labelled (Online Resource1 Fig. 2). All samples were observed by light and TEM.

Photo-conversion and transmission electron microscopy

Six to seven millilitres of the supernatant medium were carefully removed, and one part was centrifuged at 10,000×*g* for 10 min to recover all membrane material and minimise centrifugation steps. They were fixed and the remaining 3–4 ml of culture was immediately fixed without spinning. A cocktail of enzymes and sodium azide was used to avoid interference and non-specific photo-

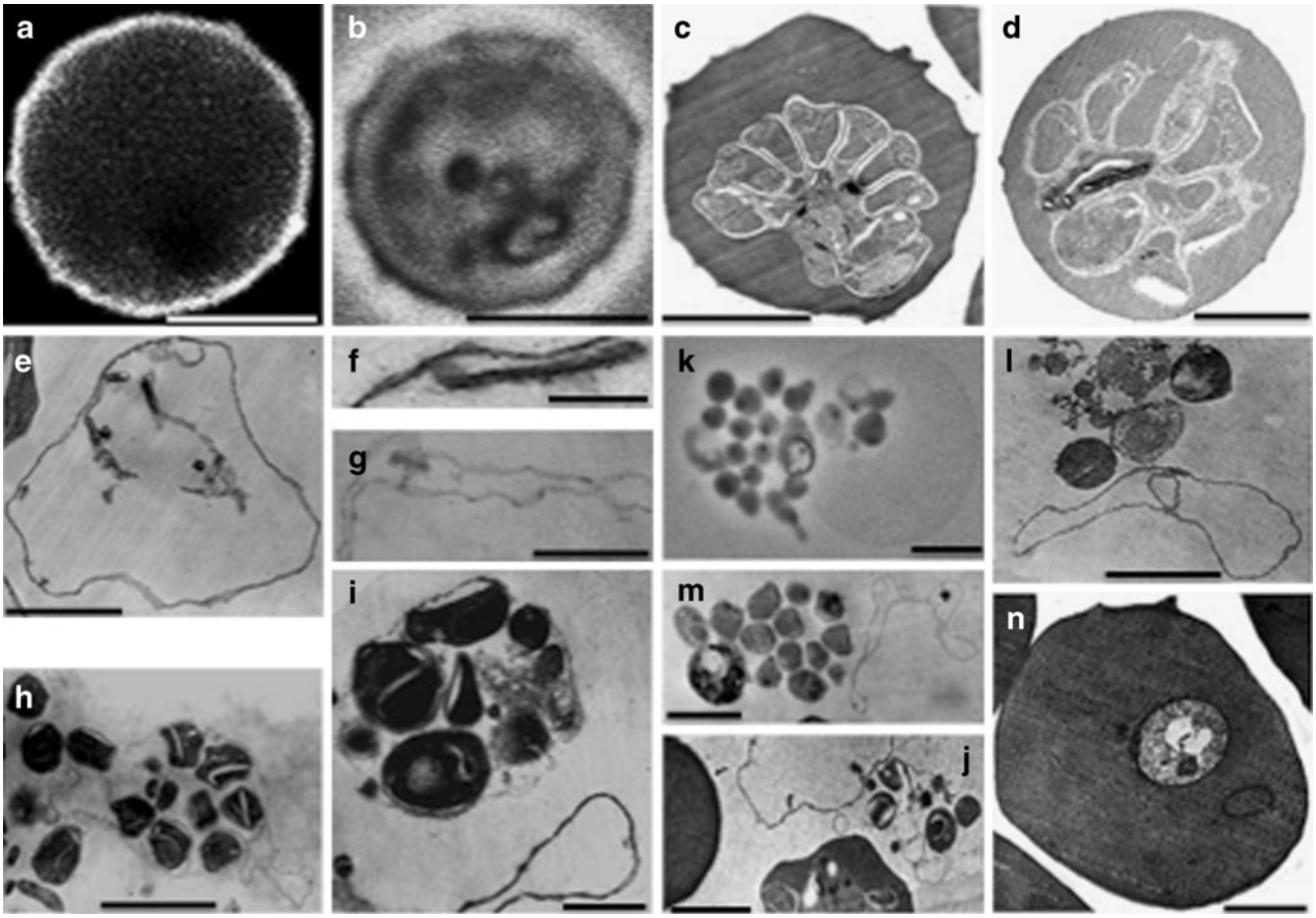

Fig. 1 Labelling infected erythrocytes with $DiIC_{16}$ and examining them by photo-conversion. Samples were prepared as described in the "Materials and methods" section. Infected erythrocytes were examined by fluorescent (**a**) and light microscopy (**b**), during maximum asexual intraerythrocytic development before merozoite release. Labelling was not associated with internal structures or the PVM (**c**). A non-photo-converted schizont from parallel control non-labelled sample after erythrocyte labelling with $DiIC_{16}$ can be observed in **d**. Note that PVM and TVM were not photo-converted in **c**. The residual body is also shown in **c** and **d**. Photo-conversion or electron-dense iE and non-iE were observed, despite the lack of contrast with 5% uranyl acetate and lead citrate. Image magnification is at 200× to 7,000×. *Scale bars* are 1.05 μm in **a**, 1,1 μm in **b** and 2 μm in **c** and **d**. Labelling Maurer's clefts in infected erythrocytes following merozoite release. Structures corresponding to Maurer's clefts inside erythrocyte ghosts became labelled with $DiIC_{16}$ as shown by the electron-dense DAB reaction product. Note the photo-converted erythrocyte remnants left behind after merozoite, release from iE (**e** and **f**). Negative controls did not show the same contrast intensity, even after photo-conversion from parallel samples non-labelled with $DiIC_{16}$ (**g**), as described in the "Materials and methods" section. **g** Non-photo-converted Maurer's cleft. Image magnification is at 7,000× to 12,000×. Merozoites still associated with each other and surrounded by a membrane could be observed during the period of merozoite release and reinvasion. **h** Clusters of merozoites still surrounded by a membrane from photo-converted samples. **i** Clusters of merozoites still surrounded by a membrane observed by TEM and close to the ghost. **j** Free merozoites in close association with vesiculated membrane. Converted, non-iE and non-converted iE. Converted ghost with structures suggestive of converted Maurer's cleft, in close association with both ghost and merozoite release. Fragments of converted membrane suggestive of PVM, related to merozoites. Image magnification is at 4,400× to 12,000×. *Scale bars* are 2.0 μm in **h** and 0.5 μm in **i** and **j**. Released merozoites were often free and close to the ghost. **k** A merozoite cluster with the residual body seemed to be closely associated with an erythrocyte ghost as observed by light microscopy. **l** Free merozoites near the ghost; note the Maurer's clefts as lamellar structures inside the ghost. **m** Free merozoites with residual body and lacking membrane bordering the cluster from unlabelled ghost were observed by TEM. Image magnification is at 200× to 7,000×. *Scale bars* are 0.5 μm in **k** and 1.0 μm in **l** and **m**. The PVM and TVM were labelled with $DiIC_{16}$ in recently reinvaded erythrocytes Examination of ring-infected erythrocytes revealed labelling of the PVM and TVM with $DiIC_{16}$ as shown by the electron-dense material. Image magnification is at 4,400×. *Scale bars* are 2.0 μm in **n**. **a** Surface-labelled mature schizont seen by fluorescence microscopy. **b** Mature schizont seen by bright/light channel. **c** Photo-converted mature schizont surface seen by TEM. **d** Mature schizont, non-labelled sample, irradiated, parallel control sample. **e** Photo-converted membrane structures and Maurer's cleft left after merozoite release from host cell. **f** Converted ghost and Maurer's cleft with knobs. **g** Irradiated, non-photo-converted control ghost with knobs. **h** Merozoite cluster released from PVM, ghost with knobs closely associates with PVM. **i** Merozoite cluster bordered by PVM, converted areas and converted ghost with knobs. **j** Panoramic non-labelled control samples shown simultaneously with labelled ones, in the same preparation. **k** Cluster of merozoites, probably released from ghost, observed by bright light microscope. Non-labelled control samples were processed simultaneously with labelled ones, in different preparations. **l** Free merozoites close to converted Maurer's cleft, ghost and converted membrane structure inside. **m** Free merozoites, residual body close to ghost. **n** Young iE, reinvaded by *Plasmodium falciparum* as control, photo-converted PVM and TVM

conversion intensity. Samples were irradiated, photo-converted and processed for TEM.

The pellet of samples to be photo-converted was fixed in 0.5% glutaraldehyde and 2% paraformaldehyde for 3 h at room temperature and spun at 7,000×*g* for 15 min. Glutaraldehyde (0.5% concentration) was used as recommended by Dantuma et al. (1998), specifically when using $DiIC_{16}$ for photo-conversion, and the remaining 3–4 ml of culture was immediately fixed in the same solution after fixation and centrifuged at 500×*g* for 10 min. Both pellets were then combined and embedded in agarose blocks (Merck low-melting temperature, type VII). One hundred micrometre sections were prepared with a vibratome (Campden Instruments Ltd); the sections were washed three times with 0.1 M HEPES pH 7.3 to remove any remaining fixative. Two more standardised fixation methods as described (Lanners 1991; Trelka et al. 2000) were used to prevent the low amount of glutaraldehyde photo-converting and compromising the ultra-structure (Online Resource1 Fig. 2).

The photo-conversion method is able to correlate light/fluorescence/electron microscopy (Cortesse et al. 2009) using different kinds of cells. iE metabolism and haemoglobin photo-oxidation could produce interference and non-specific photo-conversion intensity; peroxidases, glutathione transferases and superoxide dismutases were thus inhibited with a cocktail of 1 mM sodium azide, 1% KCN, 20 mM 3-amino-1-2-4-triazole in 0.1 M HEPES buffer, pH 7.4, for 2 h and washed (Dantuma et al. 1998) to avoid such situation. The sections were then incubated for 20 min at 0°C with 1.5 mg/ml diaminobenzidine tetrahydrochloride (DAB) in 0.1 M HEPES pH 7.5 containing the inhibitor cocktail (Maranto 1982). Haemoglobin photo-oxidation obscured other photo-conversion products when no inhibitors were used. Sections were irradiated for 20 min with a fluorescent microscope (20× lens). Fresh DAB solution was added several times during the 20-min incubation period; a non-photo-converted control section was also prepared (Fig. 1d, g, and k).

Photo-converted and non-converted control sections were fixed a second time with 1% glutaraldehyde in 0.1 M cacodylate buffer, pH 7.4, for 30 min, followed by treatment with 2% OsO_4 in 0.1 M cacodylate buffer, pH 7.4, for 1 h at room temperature and washed in the same buffer. Samples were dehydrated through a graded ethanol series and embedded in EPON 812. Thin 60 to 90 nm sections were cut using an LKB ultramichrotome, mounted on copper grids and examined with a Zeiss TEM (109 model). The samples were not stained with 5% uranyl acetate and lead citrate so that the DAB photo-conversion product could be clearly observed.

Images were taken at 3,000× to 20,000× magnification. The images were scanned using a colour image scanner (CanoScan 9950F), at 1,200 DPi resolution and altered after negatives or positives were obtained by TEM. CorelDRAW 12 and Photoshop CS3 software were used for making the changes. The positive images were adjusted with the gray scale and 300-pixel resolution; brightness, contrast, intensity and gamma values provided the final effects.

Results

The sample mainly consisted of iE containing mature schizonts, segmenters (Fig. 1a–d), membrane structures containing remnants of the iEM, having knobs (Fig. 1e–g), clusters of merozoites (Fig. 1h–j), free merozoites (Fig. 1k–m) and recently invaded erythrocytes containing early ring stages (Fig. 1n).

$DiIC_{16}$ labelling of schizont segmenter iE was only observed on the surface of iEM when the samples were examined by fluorescence microscopy (Fig. 1a and b). No evidence was found of parasite, PVM or other membrane labelling within iE.

Photo-conversion results regarding electron-dense material formation on membranes containing fluorescent lipid probes after irradiation showed electron-dense material on the iEM of labelled cells (Fig. 1c) and control unlabelled iE, but not on non-labelled and irradiated cells (Fig. 1d); this was also observed on control non-iE photo-converted and iE non-photo-converted cells found in the same field, but not on labelled and irradiated cells. Examining samples following photo-conversion revealed that small areas of fluorescent lipid probe had become incorporated into the PVM (Fig. 1j). These results indicated that labelling, the dye and the lipid analogue were not spontaneously transferred to other membranes.

No probe was transferred from iE to Maurer's clefts (MC) when the lipid analogue was inserted into iE membranes and remained there for up to 48 h of the erythrocytic cycle before merozoite release (Fig. 1a and c). Labelling was only found on iE but not on any structure within iE before merozoite release.

Released merozoites were first associated with ghosts and also MC; free merozoites were observed throughout merozoite exit and reinvasion (Fig. 1k–m). The presence of knobs in some ghosts confirmed that these membranes were derived from the iEM. TEM examination of merozoites in recently released clusters revealed that they were sometimes still surrounded by the PVM (Fig. 1h and i); they were not surrounded by the PVM at other times (Fig. 1l and m). Free merozoites lacking a surrounding PVM were predominant in most events observed; however, merozoite clusters surrounded by thin membrane were infrequently observed during merozoite release whereas both kinds of merozoites were sometimes seen to be in close association with

erythrocyte ghosts (Fig. 1h–m and Online Resource1 Fig. 2c, d).

Moreover, some erythrocyte ghosts were seen to contain photo-converted structures which were well matched to MC (Fig. 1e–g, j and l). MC became labelled with the lipid probe as indicated by electron-dense material on these membranes (Fig. 1e and f). Specific electron-dense intensity of labelling on MC was particularly notable in the photo-converted samples. The unlabelled control sample did not exhibit electron-dense material on these membranes (Fig. 1g).

Non-labelled merozoites found after merozoite release from labelled iE were corroborated by DNA staining such released merozoites for contrast (DAPI, not shown); they reinvaded non-iE which had remained labelled since the beginning of the experiments as controls and provided the signal for stopping the experiments (Fig. 1n).

The PVM and other intracytoplasmatic membranes, such as the tubovesicular membrane (TVM), were labelled with fluorescent lipids in erythrocytes which had been reinvaded by the released merozoites (Fig. 1n). iE samples and controls were processed in parallel and used in the same experimental conditions. Additional data (Online Resource1 Fig. 2 a–i) exclusively showed controls by bright light (Online Resource1 Fig. 2 a–c, f) and TEM (Online Resource1 Fig. 2 d, g–i).

Discussion

Photo-conversion was used for detecting iEM labelled with fluorescent lipid $DiIC_{16}$ to gain some insight into merozoite release at ultra-structural level. The most interesting observation in this study was the especially intense MC labelling, suggesting lipid transfer from iEM to MC during merozoite release, since MC and other associated membranes did not become labelled on contact with segmenter iE.

It was not clear how lipids were being transferred between these two membranes; one possibility was that MC became very closely associated with iEM during merozoite exit, thereby allowing for some transfer of lipids. Merozoite clusters still remained inside ghosts following merozoite release and became photo-converted. It is known that these lamellar structures are closely associated with iEM via the interaction of an MC protein, known as skeleton-binding protein (*Pf*SBP1), with the erythrocyte cytoskeleton. It has been shown that *Pf*SBP1 and MC may participate in merozoite release (Martinez et al. 1998; Blisnick et al. 2000, 2006), and it is thus possible that some lipid material is spontaneously transferred from the iEM to MC through the recruitment of some family of proteins present on iEM (Haeggstrom et al. 2004; Kaviratne et al. 2002; Blisnick et al. 2005).

One possibility that MC plays a part in merozoite release alludes to it playing some role in disrupting the iEM. For example, it has been suggested that merozoites exit as a cluster (Winograd et al. 1999) via an exit site having about 2.5 μm diameter (Winograd et al. 1999; Glushakova et al. 2005). Following merozoite exit, this opening could reseal, leaving behind the erythrocyte ghost containing clusters of merozoites, as observed in this study (Fig. 1e–g) and as previously described by Winograd et al. (1999, 2001). Interestingly, in the light of the role calcium plays in signalling pathways, Ca^{2+}-ATPase activity has been described as being associated with MC and it has been suggested that MC may contain calcium (Caldas and Wasserman 2001).

The cluster of merozoites showed the presence of a membrane, suggesting that this was the PVM surrounding merozoite clusters (Fig. 1h and i). A lack of photo-conversion was observed in most of these membranes (Fig. 1h); in spite of all samples having been irradiated, not all became photo-converted, suggesting that merozoites were being released from non-labelled iE, even though the sample had been labelled. Some fragments from the same membrane became photo-converted (Fig. 1i). Free released merozoites becoming attached to ghost erythrocytes meant that the event had occurred recently (Online Resource1 Fig. 2c) because some merozoites were still in contact with iEM (Fig. 1k, h, and j). Vesiculated membranes around them possibly corresponded to the PVM (Fig. 1j and Online Resource1 Fig. 2 d) and fragments of photo-converted darker membrane rather than vesiculated membrane suggested that this photo-converted membrane could have been part of MC, considering that these structures are a complex organelle (Wickert and Krohne 2007) which has also been described as being part of the membranous network extending from the PVM (Wickert et al. 2004).

The PVM and TVM labelled with fluorescent lipid indicated that lipids from iEM were transferred to the PVM during invasion and that the PVM was the source of the intracytoplasmic membranes found within the iE. $DiIC_{16}$ is a lipophilic non-interchangeable probe, having minimal spontaneous transfer. It is designed to see probes being transferred when distances between labelled and unlabelled membranes are extremely small; this may only occur across the aqueous space when both membranes are sufficiently tightly apposed, as proposed by Ward et al. (1993).

Additionally, labelling these intracytoplasmic membranes with the lipid indicated that they were continuous with the PVM or derived from the PVM, as previously observed by confocal microscopy (Pouvelle et al. 1994). These results also indicated that the lack of MC becoming

labelled, and that of other intraerythrocytic structures from young trophozoites to schizonts (Fig. 1 c), was not due to an inability to see the electron-dense deposits in intact iE; MC not becoming labelled indicated that they were probably non-contiguous with host erythrocyte membrane.

It should be remembered that merozoite release could be related to some PVM domains coming into contact with MC later on, since not all membranes are close to the parasite plasmatic membrane (PPM). The event could be explained by vesicles emerging from the parasite's secretory pathway becoming fused at a junction between PPM and the PVM, agreeing with Lingelbach and Przoborsky (2006) when trying to explain secretion and protein trafficking for exported proteins able to arrive at the iEM.

It has been suggested that the emergence of merozoite clusters is an artefact due to exposure to intense light (Glushakova et al. 2005) or sub-optimal conditions (Lew 2005). However, the samples prepared for TEM in this study were never exposed to intense illumination during the period of merozoite release. Likewise, the frequency at which these clusters have been observed by us and other authors (Soni et al. 2005) tends to argue against this being strictly a phenomenon arising from the prevailing conditions observed when preparations were being made. One possible explanation is that the merozoite release mechanism is not precise.

It should be considered that the sample supernatant and pellet used for studying merozoite release were mixed as described in the "Materials and methods" section, since some samples were centrifuged and others not. This means that the samples which were not close together could have been brought close together or separated or vesiculated. Nonetheless, photo-converted material such as MC was found during and around this iE event after merozoite release.

A clear understanding of malarial parasite release should focus on understanding the parasite's biology and how to inhibit the complete cycle to prevent the continuity of infection and decrease patients' sytomatology by proposing new antimalarial strategies. A detailed knowledge of the above mentioned structures, electrophysiological procedures and the use of monoclonal antibodies specifically prepared from membranes released during the in vitro culture of *P. falciparum* is thus needed (Cortes et al. 2003). Studying the events occurring when merozoites are released from *P. falciparum*-iE has been our current interest but further studies (which avoid centrifugation) aimed at identifying the proteins associated with fusion events before merozoite release and the possible mechanisms involved in it are needed for improving merozoite release characterisation. To the best of our knowledge, this is the most complete study of merozoite release from the *Plasmodium* malaria parasite at ultra-structural level and also the first report of $DiIC_{16}$ labelling and conversion to an electro-dense precipitate analysed by TEM following fluorescence microscopy studies during *Plasmodium* merozoite release.

Acknowledgements This work was financed by the Instituto Nacional de Salud, Bogotá, Colombia, and the Instituto Colombiano para el Desarrollo de la Ciencia y la Tecnología (COLCIENCIAS—project no. 110140820398 and COLCIENCIAS—project 2104-05-018-97) and Universidad Nacional de Colombia, (Medicine Faculty), Bogotá, project no. 201010011388. We would like to thank the Universidad Nacional de Colombia's Public Health and Tropical Medicine Department and Institute of Biotechnology PhD studies (Science Faculty) for providing the research facilities. We would also like to thank Dr. Marcela Camacho, Biology Department, Universidad Nacional de Colombia, head of the Biophysics and Biology of Membranes Research Group of International Centre of Physics (CIF) Biophysics laboratory, for her helpful discussion. We extend our gratitude to Dr. Mark F. Wiser for his valuable suggestions, Dr. Enrique Winograd for originally proposing the study of merozoite release and Dr. Hugo D. Lujan for his important final comments and advice (Biochemistry and Molecular Biology Laboratory, Medicine Faculty, Universidad Católica de Córdoba).

References

Blisnick T, Morales BM, Barale JC, Uzureau P, Berry L, Desroses S, Fujioka H, Mattei D, Braun BC (2000) *Pf*sbp1, a Maurer's cleft *Plasmodium falciparum* protein, is associated with the erythrocyte skeleton. Mol Biochem Parasitol 111:107–121

Blisnick T, Vincensini L, Barale JC, Namane A, Braun-Breton C (2005) LANCL1, an erythrocyte proteins recruited to the Maurer's clefts during *Plasmodium falciparum* development. Mol Biochem Parasitol 141:39–47

Blisnick TL, Vincensini GF, Braun BC (2006) Protein phosphotase 1, a *Plasmodium falciparum* essential enzyme, is exported to the host cell and implicated in the release of infectious merozoites. Cell Microbiol 8:591–601

Caldas ML, Wasserman M (2001) Cytochemical localisation of calcium ATPase activity during the erythrocytic cell cycle of *Plasmodium falciparum*. Int J Parasitol 31:776–782

Clavijo CA, Mora CA, Winograd E (1998) Identification of novel membrane structures in *Plasmodium falciparum*-infected erythrocytes. Mem Inst Oswaldo Cruz 93:115–120

Cohen F, Melykian GB (1998) Methodologies in the study of cell fusion. Methods: a companion to Meths. Enzymiol 16:215–226

Cortes GT, Winograd E, Wiser MF (2003) Characterization of proteins localized to a subcellular compartment associated with an alternate secretory pathway of the malaria parasite. Mol Biochem Parasitol 129:127–135

Cortesse K, Diaspro A, Tacchetti C (2009) Advanced correlative light/electron microscopy: current methods and new developments using Tokuyasu cryosections. J Histochem Cytochem 57:1103–1112

Cowman AF, Crabb BS (2006) Invasion of red blood cells by malaria parasites. Cell 124:755–766

Dantuma NP, Pijnenburg MA, Diederen JHB, Van der Hors DJ (1998) Electron microscopic visualization of receptor-mediated endocytosis of dil-labelled lipoproteins by diaminobenzidine photoconversion. J Histochem Cytochem 46:1085–1090

Dvorak JA, Miller LH, Whitehouse WC, Shiroishi T (1975) Invasion of eyrthrocytes by malaria merozoites. Science 187:748–750

Glushakova S, Yin TD, Zimmerberg J (2005) Membrane transformation during malaria parasite release from human red blood cells. Curr Biol 15:1645–1650

Glushakova S, Mazar J, Hohmann Marriott MF, Hama E, Zimmerberg J (2009) Irreversible effect of cysteine protease inhibitors on the release of malaria parasites from infected erythrocytes. Cell Microbiol 11:95–105

Glushakova S, Humphrey G, Leikina E, Balaban A, Miller J, Zimmerberg J (2010) New stages in the program of malaria parasite egress imaged in normal and sickle erythrocytes. Curr Biol 20:1117–1121

Haeggstrom M, Kironde F, Berzins K, Chen Q, Wahlgren M, Fernández V (2004) Common trafficking pathway for variante antigens destined for the surface of the *Plasmodium falciparum*-infected erythrocyte. Mol Biochem Parasitol 133:1–14

Haldar K, Uyetake L (1992) The movement of fluorescent endocytic tracers in *Plasmodium falciparum*-infected erythrocytes. Mol Biochem Parasitol 50:161–178

Haldar K, Uyetake L, Ghori N, Elmendorf HG, Li WL (1991) The accumulation and metabolism of a fluorescent ceramide derivative in *Plasmodium falciparum*-infected erythrocytes. Mol Biochem Parasitol 49:143–156

Jensen JB (1978) Concentration from continuous culture of erythrocytes infected with trophozoites and schizonts of *Plasmodium falciparum*. Am J Trop Med Hyg 27:1274–1276

Kaviratne MS, Khan M, Jarra W, Preiser PR (2002) Small variant STEVOR antigen is uniquely located within Maurer's clefts in *Plasmodium falciparum*-infected red blood cells. Eukaryot Cell 1:926–935

Lambros C, Vanderberg JP (1979) Synchronization of *Plasmodium falciparum* erythrocytic stages in culture. J Parasitol 65:418–420

Lanners HN (1991) Ultrastructure of erythrocytes from Aotus trivirgatus and Saimiri sciureus monkeys infected by *Plasmodium vivax*. Parasitol Res 77:395–401

Lew VL (2005) Malaria: endless fascination with merozoite release. Curr Biol 15:R760–R761

Lingelbach K, Przoborsky JM (2006) The long and winding road: protein trafficking mechanisms in the Plasmodium falciparum infected erythrocyte. Mol Biochem Parasitol 147:1–8

Maranto A (1982) Neuronal mapping: a photooxidation reaction makes lucifer yellow useful for electron microscopy. Science 17:953–955

Martinez SL, Clavijo CA, Winograd E (1998) Identification of peripheral membrane proteins associated with the tubo vesicular network of *Plasmodium falciparum* infected erythrocytes. Mol Biochem Parasitol 91:273–280

Pouvelle B, Gormley JA, Tarashi TF (1994) Characterization of trafficking pathways and membrane genesis in malaria infected erythrocytes. Mol Biochem Prasitol 66:83–96

Rayner JC (2006) Erythrocyte exit: out, damned merozoite! Out I say! Trends Parasitol 22:1889–192

Salmon BL, Oksman A, Goldberg DE (2001) Malaria parasite exit from the host erythrocyte: a two step process requiring extraerythrocytic proteolysis. Proc Natl Acad Sci USA 98:271–276

Soni S, Dhawan S, Rosen KM, Chafel M, Chishti AH, Hanspal M (2005) Characterization of events preceding the release of malaria parasite from the host red blood cell. Blood Cells Mol Dis 35:201–211

Trager W (2002) On the release of malaria merozoites. Trends Parasitol 18:60–61

Trager W, Jensen JB (1976) Human malaria parasites in continuous culture. Science 193:673–675

Trelka DP, Schneider TG, Reeder JC, Taraschi TF (2000) Evidence for vesicle-mediated trafficking of parasite proteins to the host cell cytosol and erythrocyte surface membrane in *Plasmodium falciparum* infected erythrocytes. Mol Biochem Parasitol 106:131–145

Ward GE, Miller LH, Dvorak A (1993) The origin of parasitophorous vacuole membrane lipids in malaria-infected erythrocytes. J Cell Sci 106:237–248

Wickert H, Krohne G (2007) The complex morphology of Maurer's cleft: from discovery to three-dimensional reconstruction. Trends Parasitol 23:502–509

Wickert H, Göttler W, Krohne G, Lanzer M (2004) Maurer's cleft organization in the cytoplasm of *Plasmodium falciparum*-infected erythrocytes: new insights from three-dimensional reconstruction of serial ultrathin sections. Eur J Cell Biol 83:567–582

Wickham ME, Culvenor JG, Cowman AF (2003) Selective inhibition of a two-step egress of malaria parasites from the host erythrocyte. J Biol Chem 278:37658–37663

Winograd E, Clavijo CA, Bustamante LY, Jaramillo M (1999) Release of merozoites from *Plasmodium falciparum*-infected erythrocytes could be mediated by a non-explosive event. Parasitol Res 85:621–624

Winograd E, Robles WM, Caldas ML, Cortes GT (2001) Cytoadherence of the malaria-infected erythrocyte membrane to C32 melanoma cells after merozoites are released from parasitized infected cells. Parasitol Res 87:264–268